TÜBİTAK

Turkish Journal of Chemistry

http://journals.tubitak.gov.tr/chem/

Research Article

Turk J Chem
(2021) 45: 17-25
© TÜBİTAK
doi:10.3906/kim-2007-47

Synthesis of nonperipherally tetra-[5-(diethylamino)-2-formylphenoxy] substituted metallophthalocyanines and their electrochemistry

Turgut KELEŞ[1], Dilek ÜNLÜER[2], Zekeriya BIYIKLIOĞLU[2,*], Yasemin ÜNVER[2]
[1]Central Research Laboratory Application and Research Center, Recep Tayyip Erdoğan University, Rize, Turkey
[2]Karadeniz Technical University, Department of Chemistry, Trabzon, Turkey

Received: 23.07.2020 • **Accepted/Published Online:** 25.09.2020 • **Final Version:** 17.02.2021

Abstract: 3-[5-(diethylamino)-2-formylphenoxy]phthalonitrile (**n-TY-CN**), metallophthalocyanines **n-TY-Co**, **n-TY-Cu**, and **n-TY-Mn** bearing [5-(diethylamino)-2-formylphenoxy] groups at nonperipheral positions were prepared for the first time. These compounds were characterized with IR, NMR (only for **n-TY-CN**), mass and UV-vis (except **n-TY-CN**) spectroscopy. Voltammetric characterizations of **n-TY-Co**, **n-TY-Cu**, and **n-TY-Mn** revealed that while **n-TY-Co**, **n-TY-Cu**, and **n-TY-Mn** showed characteristic Pc ring and/or metal-based reduction reaction, **n-TY-Co**, **n-TY-Cu**, and **n-TY-Mn** were coated on the working electrode during the oxidation processes owing to the cationic electropolymerizations of the [5-(diethylamino)-2-formylphenoxy] substituents.

Key words: Synthesis, diethylamino, phthalocyanine, electrochemistry

1. Introduction

Phthalocyanines are all-purpose and durable compounds [1]. They have an extended π-conjugation system and different types of central metals [2]. In addition, their unique electronic and chemical properties, physical and optical properties, as well as chemical flexibility allow for the preparation of a variety of related structures and diverse applications ranging from industrial to biological areas [3,4]. Phthalocyanines have been used in different areas such as photodynamic therapy [5,6], nonlinear optical materials [7], electrochemical sensors [8,9], biosensors [10], solar cells [11,12], light-emitting devices [13], liquid crystals [14], electrocatalysts [15], and electropolymerization [16,17]. The solubility of unsubstituted phthalocyanines is very low in organic solvents. This condition affects the use of phthalocyanines in many areas. The solubility of phthalocyanines can be increased with substitution of phenoxy, alkyl, alkoxy, long chain, and bulky groups at peripheral, nonperipheral, or axial positions of the phthalocyanine [18–20]. Diethylamino groups can be used in many applications such as anticancer agents [21], DNA interactions [22], and photodynamic therapy [23]. In addition, the electrochemical features of diethylamino groups are significant. In the literature, it is shown that the introduction of diethylamino groups into the peripheral/nonperipheral positions of phthalocyanines increased their electrochemical and electropolymerization properties [24–27]. Here, we wondered how the presence of phthalocyanines in the nonperipheral positions of the diethylamino group affects the electrochemical properties of phthalocyanine compounds. For this reason, in this work, we combined these two functional compounds (diethylamino and phthalocyanine) into a single compound. In this study, we have synthesized nonperipherally tetra-[5-(diethylamino)-2-formylphenoxy] substituted **n-TY-Co**, **n-TY-Cu**, and **n-TY-Mn**, and investigated their electrochemical properties.

2. Experimental details

Information about equipment, materials, and electrochemistry experiments is provided in the Supplementary Information section.

2.1. Synthesis

2.1.1. 3-[5-(diethylamino)-2-formylphenoxy]phthalonitrile (n-TY-CN)

4-(diethylamino)-2-hydroxybenzaldehyde (1 g, 5.2 mmol), 3-nitrophthalonitrile (0.9 g, 5.2 mmol), and dry K_2CO_3 (2.15 g, 15.6 mmol) were dissolved in DMF (15 mL) at 55 °C under nitrogen atmosphere for 96 h. Then, the solution was estranged

* Correspondence: zekeriyab@ktu.edu.tr

and spilled into iced water (200 mL). **n-TY-CN** was crystallized from ethanol and purified using column chromatography on aluminum oxide with chloroform. Yield: 0.47 g (33%), m.p. 155–157 °C. IR (ATR), ν/cm^{-1}: 3097 (Ar–H), 2974–2877 (Aliph. C–H), 2225 (C≡N), 1674 (C=O), 1603, 1543, 1445, 1377, 1260, 1192, 1094, 1074, 844, 799, 689. ^{1}H NMR (400 MHz, DMSO-d_6), (δ): 9.71 (s, 1H, =CH), 7.81–7.73 (m, 3H, Ar–H), 7.21 (d, 1H, Ar–H), 6.78 (d, 1H, Ar–H), 6.52 (s, 1H, Ar–H), 3.46–3.41 (m, 4H, CH_2–N), 1.10 (t, 6H, CH_3). ^{13}C-NMR (100 MHz, DMSO-d_6), (δ): 185.97, 160.97, 156.84, 154.05, 136.34, 133.73, 128.13, 121.15, 116.17, 116.07, 115.46, 113.94, 109.59, 104.91, 103.36, 44.67, 12.73. MS (ESI), (m/z) calcl. 319; found: 342.03 $[M + Na]^+$.

2.1.2. 1(4),8(11),15(18),22(25)-tetrakis-[5-(diethylamino)-2-formylphenoxy]-phthalocyaninato cobalt (II) (n-TY-Co)
3-[5-(diethylamino)-2-formylphenoxy]phthalonitrile (150 mg, 0.36 mmol), $CoCl_2$ (24 mg, 0.18 mmol), 1-pentanol (2.5 mL), and DBU (3 drops) were stirred at 160 °C for 24 h under N_2 atmosphere. The product was precipitated with hexane. **n-TY-Co** was obtained by column chromatography using basic aluminum oxide and $CHCl_3$ as a solvent. Yield: 27 mg (17%), m.p. > 300 °C. IR (ATR), ν/cm^{-1}: 3066 (Ar–H), 2959–2852 (Aliph. C–H), 1667 (C=O), 1590, 1517, 1400, 1353, 1238, 1196, 1136, 1090, 985, 797, 746, 692. UV-vis (THF) λ_{max} nm (log ε): 678 (5.02), 621 (4.48), 311 (5.06). MALDI-TOF-MS (DIT) m/z: 1336.04 $[M]^+$, 1508.00 $[M + DIT–C_4H_6]^+$, 1612.48 $[M + DIT + 3H_2O–4H]^+$, 1697.22 $[M + DIT + 3K + H_2O]^+$.

2.1.3. 1(4),8(11),15(18),22(25)-tetrakis-[5-(diethylamino)-2-formylphenoxy]-phthalocyaninato copper (II) (n-TY-Cu)
n-TY-Cu was synthesized similarly to **n-TY-Co** by using $CuCl_2$ instead of $CoCl_2$. Yield: 40 mg (38%), m.p. > 300 °C. IR (ATR), ν/cm^{-1}: 3065–3035 (Ar–H), 2967–2867 (Aliph. C–H), 1664 (C=O), 1590, 1519, 1480, 1397, 1330, 1235, 1194, 1124, 1078, 890, 799, 742, 630. UV-vis (THF) λ_{max} nm (log ε): 697 (5.03), 662 (4.36), 629 (4.35), 340 (4.87). MALDI-TOF-MS (CHCA) m/z: 1250.11 $[M–C_6H_{17}]^+$, 1319.48 $[M–CH_8]^+$, 1339.70 $[M]^+$, 1402.70 $[M + Na + K + H]^+$, 1425.63 $[M + 2Na + K + H]^+$, 1511.27 $[M + CHCA–H_2O + H]^+$.

2.1.4. 1(4),8(11),15(18),22(25)-tetrakis-[5-(diethylamino)-2-formylphenoxy]-phthalocyaninato manganese (III) chloride (n-TY-Mn)
n-TY-Mn was synthesized similarly to **n-TY-Co** by using $MnCl_2$ instead of $CoCl_2$. Yield: 40 mg (37%), m.p. > 300 °C. IR (ATR), ν/cm^{-1}: 3060 (Ar–H), 2965–2856 (Aliph. C–H), 1663 (C=O), 1594, 1518, 1482, 1326, 1239, 1093, 1067, 1013, 894, 797, 741, 692. UV-vis (THF) λ_{max} nm (log ε): 795 (4.78), 755 (4.95), 527 (4.36), 345 (5.20). MALDI-TOF-MS (DIT) m/z: 1308.54 $[M–C_4H_{11}]^+$, 1331.85 $[M–Cl–H]^+$, 1348.80 $[M–CH_7]^+$, 1417.65 $[M + 2Na + K–Cl]^+$.

3. Results and discussion

3.1. Synthesis and characterization

In this study, 3-[5-(diethylamino)-2-formylphenoxy]phthalonitrile (**n-TY-CN**), nonperipherally tetra-[5-(diethylamino)-2-formylphenoxy] substituted metallophthalocyanines **(n-TY-Co**, **n-TY-Cu**, **n-TY-Mn)** were synthesized for the first time and characterized with IR, NMR (only for **n-TY-CN**), mass and UV-vis (except **n-TY-CN**) spectroscopy. The synthesis of **n-TY-Co**, **n-TY-Cu**, and **n-TY-Mn** is shown in Figure 1. The detailed synthesis of 3-[5-(diethylamino)-2-formylphenoxy] phthalonitrile (**n-TY-CN**) and metallophthalocyanines (**n-TY-Co**, **n-TY-Cu**, **n-TY-Mn**) is given in Supplementary Information. Stretching vibrations of C=N groups at 2225 cm^{-1} were observed in the IR spectrum of **n-TY-CN**. In ^{1}H-NMR spectrum of **n-TY-CN**, aldehyde and aromatic protons were detected at 9.71 and 7.81–6.52 ppm. Also, the aliphatic CH_2–N and –CH_3 protons were observed at 3.46–3.41 ppm as a multiplet, 1.10 ppm as a triplet. The aromatic and aliphatic carbon signals were observed at 185.97–103.36 and 44.67–12.73 ppm. In the IR spectra of **n-TY-Co**, **n-TY-Cu**, and **n-TY-Mn**, the sharp C≡N stretching vibration disappeared. Also, C=O stretching vibrations of **n-TY-Co**, **n-TY-Cu**, and **n-TY-Mn** were shown at 1667, 1664, and 1663 cm^{-1}, respectively. NMR spectra of **n-TY-Co**, **n-TY-Cu**, and **n-TY-Mn** could not be obtained owing to paramagnetic Co(II), Cu(II), Mn(III) ions [28]. MALDI-TOF mass spectra were obtained in dithranol (DIT) for **n-TY-Co, n-TY-Mn**, and alpha-cyano4-hydroxycinnamic acid (CHCA) for **n-TY-Cu** as MALDI matrix materials. The molecular ion peaks of **n-TY-CN, n-TY-Co**, **n-TY-Cu**, and **n-TY-Mn** were observed as 342.03 $[M + Na]^+$, 1336.04 $[M]^+$, 1339.70 $[M]^+$, and 1331.85 $[M–Cl–H]^+$, respectively (Figure 2). In the UV-vis spectra of **n-TY-Co**, **n-TY-Cu**, and **n-TY-Mn** in THF, the characteristic Q band (678 nm for **n-TY-Co**, 697 nm for **n-TY-Cu**, 795 nm for **n-TY-Mn**) and B band (311 nm for **n-TY-Co**, 340 nm for **n-TY-Cu**, 345 nm for **n-TY-Mn**) were observed (Figure 3). As shown in Figure 3, **n-TY-Mn** showed aggregation in THF, but **n-TY-Co** and **n-TY-Cu** did not show any aggregation in THF.

3.2. Voltammetric studies

Voltammetric analysis of **n-TY-Co**, **n-TY-Cu**, and **n-TY-Mn** was achieved in DCM using a (DCM)/(TBAP) electrolyte system on a Pt working electrode. The voltammetric data is shown in Table. Figures 4a and 4b show the CV and SWV responses of **n-TY-Co**, **n-TY-Cu**, and **n-TY-Mn**. As shown in Figure 4, **n-TY-Co** showed metal-based reversible and Pc-based quasireversible reduction reactions labeled as R_1 ($E_{1/2}$ = –0.33 V), R_2 ($E_{1/2}$ = –1.53 V). Also, **n-TY-Cu** gave two

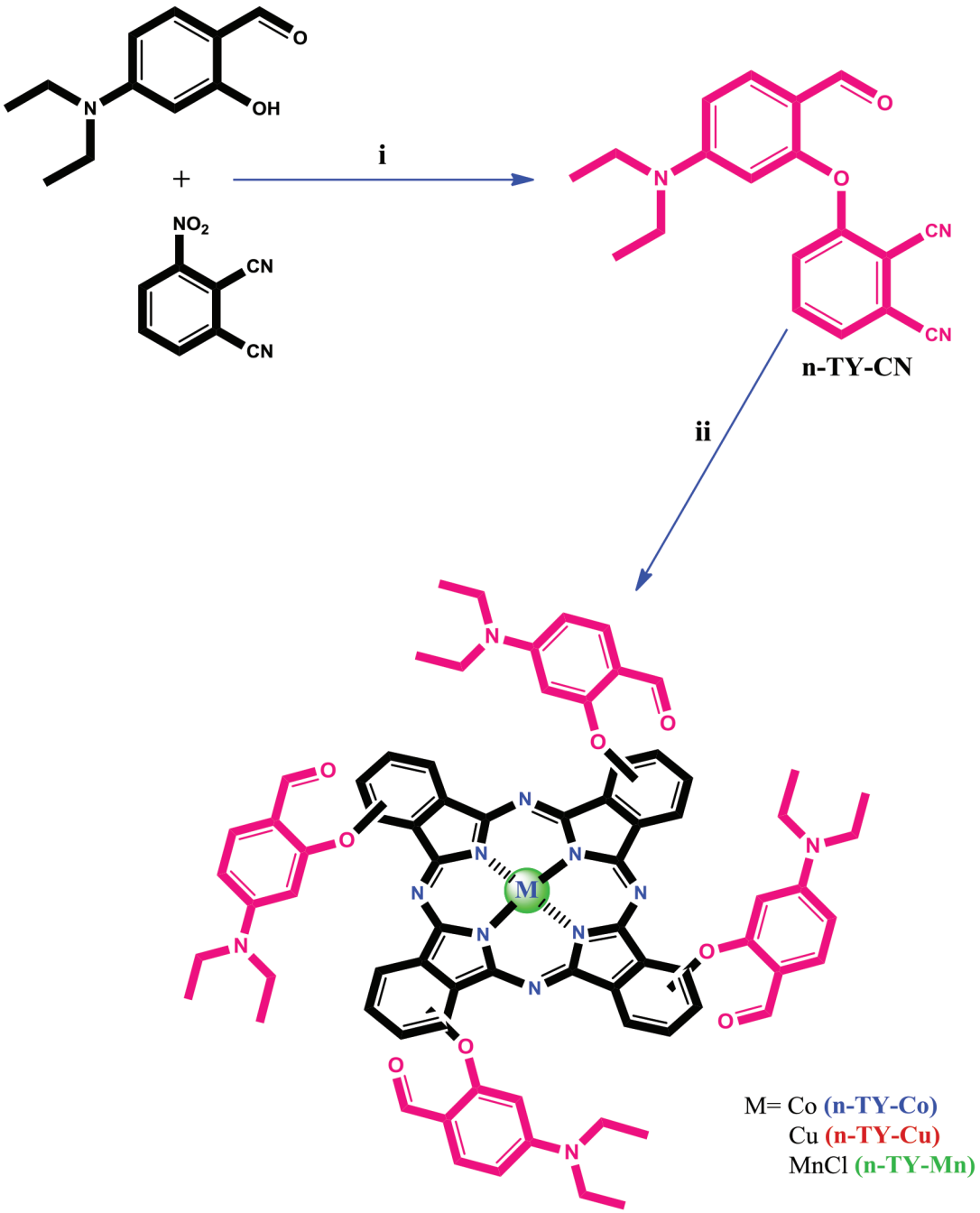

Figure 1. The synthesis of **n-TY-Co, n-TY-Cu,** and **n-TY-Mn** containing [5-(diethylamino)-2-formylphenoxy] groups. (i) DMF, K_2CO_3, 55 °C; (ii) n-pentanol, DBU, metal salts, 160 °C.

reversible, Pc-based reduction reactions ($E_{1/2}$ = –0.82 V, –1.25 V). On the other hand, **n-TY-Mn** illustrated reversible (R_1 $E_{1/2}$ = –0.13 V) and quasireversible (R_2 $E_{1/2}$ = –0.97 V, R_3 $E_{1/2}$ = –1.46 V) reduction processes, which were assigned to $[Cl–Mn^{III}Pc^{-2}]$ / $[Cl–Mn^{II}Pc^{-2}]^{-1}$, $[Mn^{II}Pc^{-2}]$ / $[Mn^{I}Pc^{-2}]^{-1}$, $[Mn^{I}Pc^{-2}]^{-1}$ / $[Mn^{I}Pc^{-3}]^{-2}$ couples. The ligands containing diethylamino groups polymerize during the oxidation reaction [29,30]. For this reason, **n-TY-Co**, **n-TY-Cu**, and **n-TY-Mn** containing [5-(diethylamino)-2-formylphenoxy] groups were electropolymerized during the oxidation reaction. Figure 5 shows the CV responses of **n-TY-Co**, **n-TY-Cu**, and **n-TY-Mn** during repetitive CV cycles. Figure 5a shows the repetitive CV responses of the **n-TY-Co** recorded at 0.100 V s^{-1} scan rate within a positive potential window of DCM/

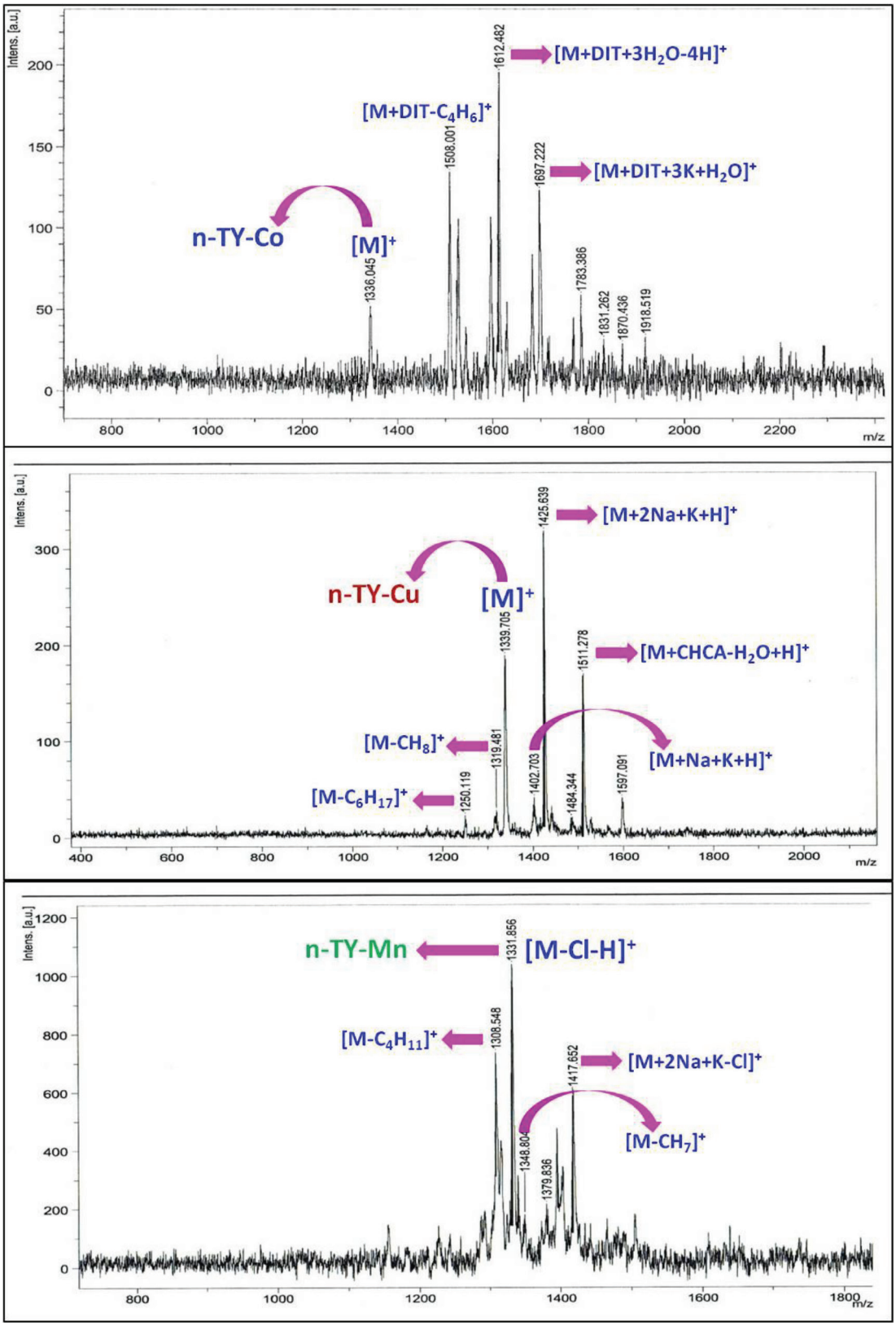

Figure 2. MALDI-TOF MS spectrum of **n-TY-Co**, **n-TY-Cu**, and **n-TY-Mn**.

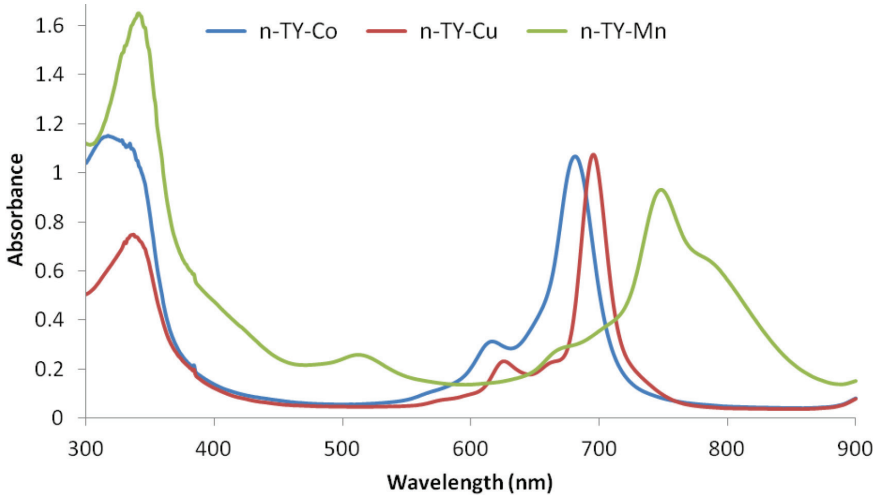

Figure 3. UV-vis spectra of **n-TY-Co, n-TY-Cu**, and **n-TY-Mn** in THF.

Table. Electrochemical results of the **n-TY-Co, n-TY-Cu, n-TY-Mn**. All data were given versus SCE.

Pcs		Oxidation of substituent		R_1	R_2	R_3
n-TY-Co	$^aE_{1/2}$	0.81	1.18	–0.33	–1.53	-
n-TY-Cu	$^aE_{1/2}$	1.05	-	–0.82	1.25	-
n-TY-Mn	$^aE_{1/2}$	1.10	-	–0.13	–0.97	–1.46

[a]: $E_{1/2}$ values $((E_{pa}+E_{pc})/2)$ were given versus SCE at 0.100 V s^{-1} scan rate.

TBAP. During the first anodic CV cycle, **n-TY-Co** shows two oxidation peaks at 0.81 and 1.18 V. During the second to fifteenth CV cycles, the anodic waves increase with potential shifts at 0.92 and 1.27 V. After this point, the potentials decrease with the ultimate disappearance of current intensity after the 20th cycle. Figure 5b illustrates CV responses of **n-TY-Cu** during repetitive CV cycles. During the first anodic scan, an anodic wave at 1.05 V and its reverse cathodic couple is recorded at 0.92 V. During the second to seventeenth CV cycles, the anodic waves increase with a potential shift at 1.20 V. Also, during the consecutive third CV cycle, two new cathodic waves are recorded at 0.48 and 0.89 V. These new waves increase in current intensity with a negative potential shift to 0.33 and 0.84 V during the 20th CV cycle. Figure 5c shows the repetitive CV cycles **n-TY-Mn**. During the first CV cycle, an oxidation peak at 1.10 V is observed. During the second to ninth CV cycles, this peak increases in current intensity with a positive potential shift. After this point, the potentials decrease with the ultimate disappearance of current intensity after the 20th cycle. These voltammetric responses show the electropolymerization of the **n-TY-Co**, **n-TY-Cu**, and **n-TY-Mn** on the working electrode due to the oxidation of diethylamino groups of the metallophthalocyanines. In order to prepare a composite electrode, electropolymerization is required [31]. Also, electropolymerization necessitates electroactive groups, for example, morpholine [32], diethylamino [33], and thiophene [34] in the monomer system. For these reasons, the electropolymerization feature may allow the synthesized phthalocyanines (**n-TY-Co**, **n-TY-Cu**, **n-TY-Mn**) to be used in different electrochemical areas, for example as electrocatalyts, electrochromic materials, and electrochemical sensors [35].

4. Conclusion

In this work, nonperipherally tetra-[5-(diethylamino)-2-formylphenoxy] substituted **n-TY-Co**, **n-TY-Cu**, and **n-TY-Mn** were synthesized and characterized. Voltammetric analysis of **n-TY-Co**, **n-TY-Cu**, **n-TY-Mn** was defined by using cyclic and square wave voltammetry. Voltammetric results show that **n-TY-Co** and **n-TY-Cu** give two reduction processes, but **n-TY-Mn** gives three reduction processes during the cathodic scans. Also, **n-TY-Co**, **n-TY-Cu**, and **n-TY-Mn** revealed electropolymerization responses during the anodic scans because the ligands containing [5-(diethylamino)-2-formylphenoxy] groups polymerize during the oxidation reaction.

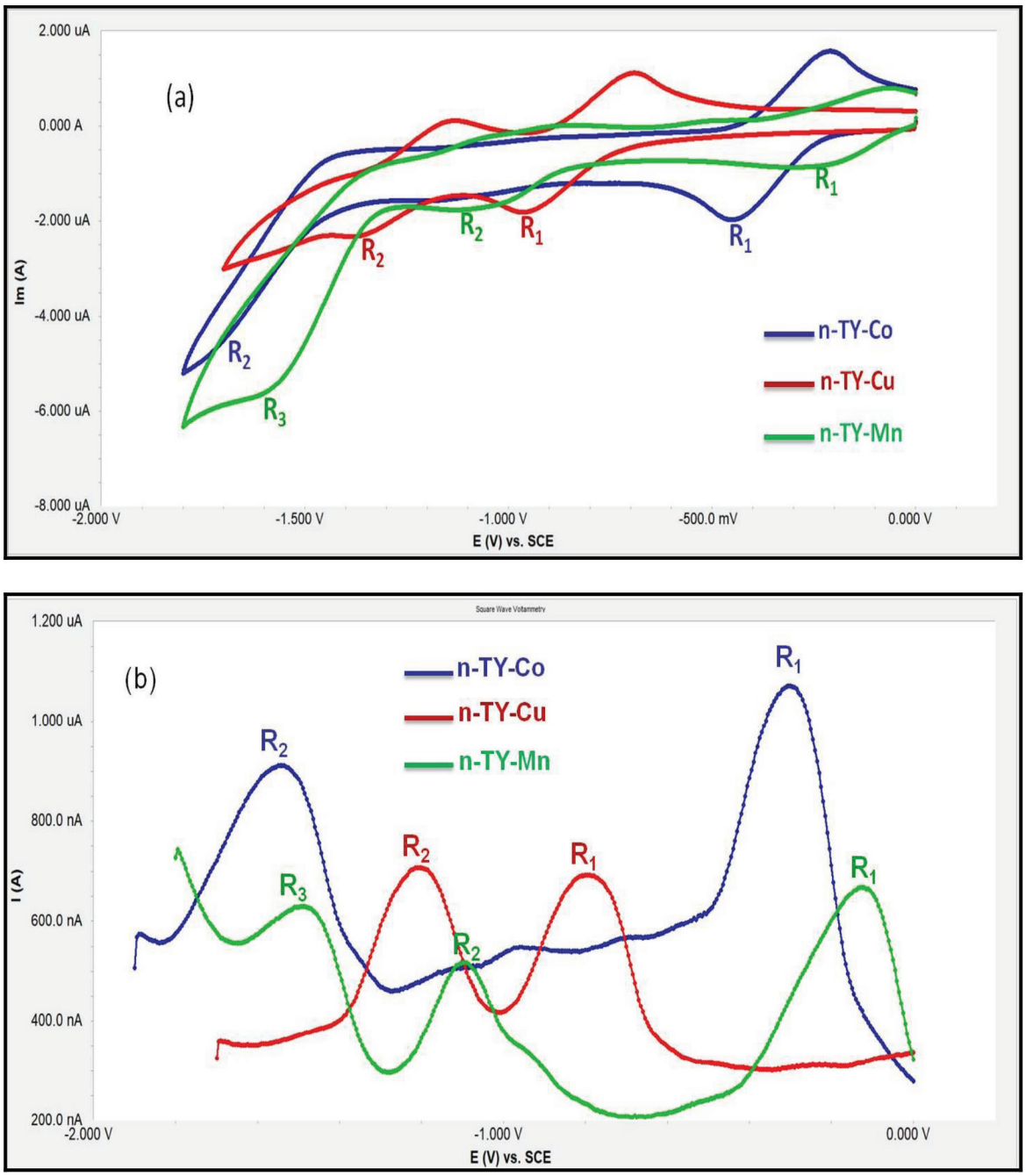

Figure 4. (a) CV graph of **n-TY-Co**, **n-TY-Cu**, and **n-TY-Mn** in TBAP/DCM electrolyte system on platin working electrode. (b) SWV graph of **n-TY-Co, n-TY-Cu,** and **n-TY-Mn** in TBAP/DCM electrolyte system on platin working electrode.

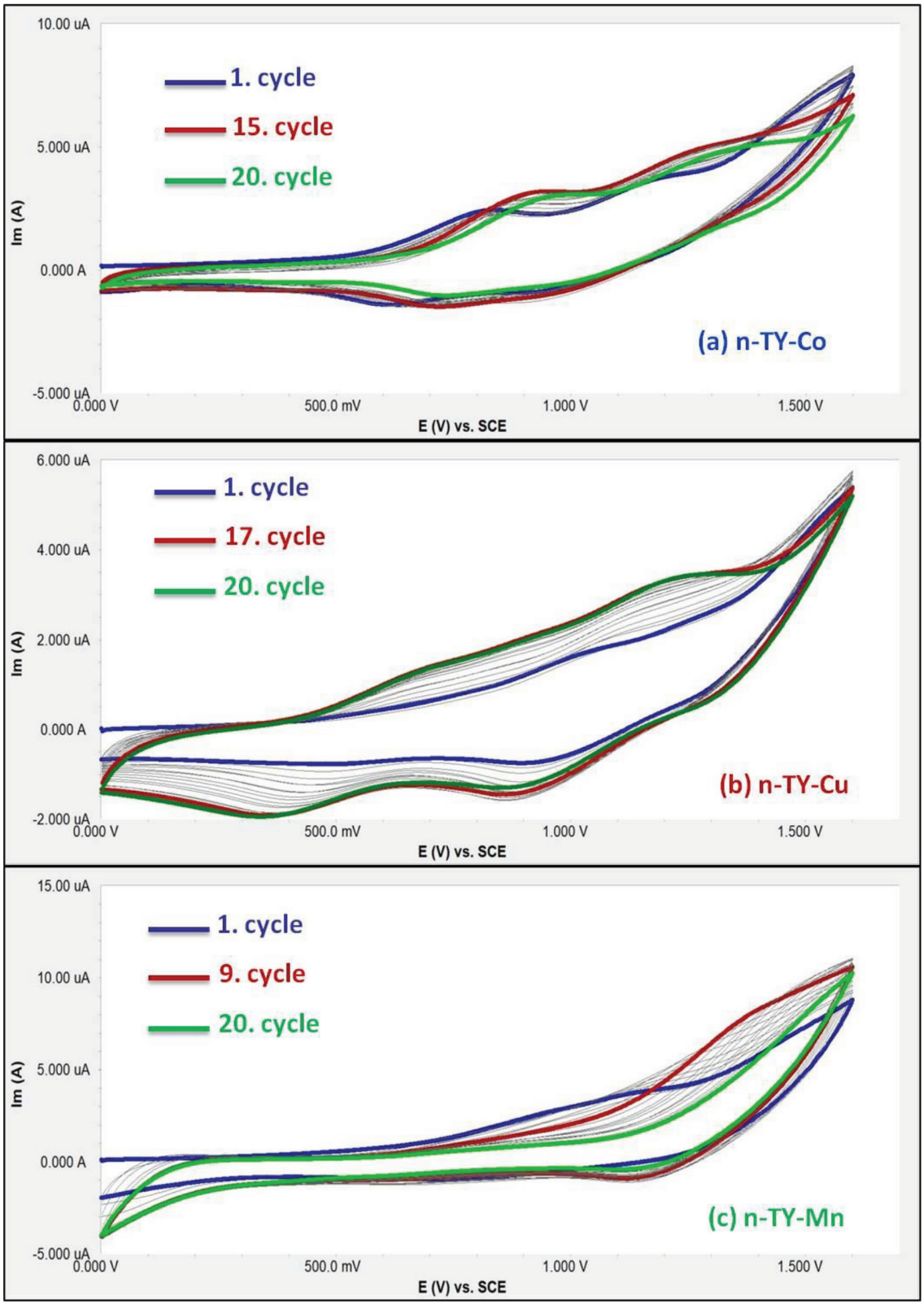

Figure 5. (a) Repetitive CVs of **n-TY-Co** in TBAP/DCM electrolyte system on platin working electrode at 0.100 mV s^{-1} scan rate. (b) Repetitive CVs of **n-TY-Cu** in TBAP/DCM electrolyte system on platin working electrode at 0.100 mV s^{-1} scan rate. (c) Repetitive CVs of **n-TY-Mn** in TBAP/DCM electrolyte system on platin working electrode at 0.100 mV s^{-1} scan rate.

References

1. Sekhosana KE, Shumba M, Nyokong T. Electrochemical and non-linear optical behavior of a new neodymiumdouble-decker phthalocyanine. Polyhedron 2017; 138: 154-160.
2. Filippova A, Vashurin A, Znoyko S, Kuzmin I, Razumov M et al. Novel Co(II) phthalocyanines of extended periphery and their water-soluble derivatives. Synthesis, spectral properties and catalytic activity. Journal of Molecular Structure 2017; 1149: 17-26.
3. Tejerina L, Caballero E, Martinez-Diaz MV, Nazeeruddin MK, Gratzel M et al. Introducing rigid π-conjugated peripheral substituents in phthalocyanines for DSSCs. Journal of Porphyrins and Phthalocyanines 2016; 20: 1361-1367.
4. Güngör Ö, Altınbaş GÖ, Durmuş M, Ahsen V. The effect of "on/off" molecular switching on the photophysical and photochemical properties of axially calixarene substituted actIVatable silicon(IV)phthalocyanine photosensitizers. Dalton Transactions 2016; 45: 7634-7641.
5. Ogbodu RO, Nitzsche B, Ma A, Atilla D, Gürek AG et al. Photodynamic therapy of hepatocellular carcinoma using tetra-triethyleneoxysulfonyl zinc phthalocyanine as photosensitizer. Journal of Photochemistry and Photobiology B: Biology 2020; 208: 111915.
6. Ömeroğlu İ, Göksel M, Kussovski V, Mantareva V, Durmuş M. Novel water-soluble silicon(IV) phthalocyanine for photodynamic therapy and antimicrobial inactivations. Macroheterocycles 2019; 12: 255-263.
7. Majeed SA, Nwaji N, Mack J, Nyokong T, Makhseed S. Nonlinear optical responses of carbazole-substituted phthalocyanines conjugated to graphene quantum dots and in thin films. Journal of Luminescence 2019; 213: 88-97.
8. Porto LS, da Silva DN, Silva MC, Pereira AC. Electrochemical sensor based on multi-walled carbon nanotubes and cobalt phthalocyanine composite for pyridoxine determination. Electroanalysis 2019; 31: 820-828.
9. Keleş T, Akyüz D, Bıyıklıoğlu Z, Koca A. Electropolymerization of metallophthalocyanines carrying redox active metal centers and their electrochemical pesticide sensing application. Electroanalysis 2017; 29: 2125-2137.
10. Attia MS, Ali K, El-Kemary M, Darwish WM. Phthalocyanine-doped polystyrene fluorescent nanocomposite as a highly selective biosensor for quantitative determination of cancer antigen 125. Talanta 2019; 201: 185-193.
11. Yıldız B, Güzel E, Akyüz D, Arslan BS, Koca A et al. Unsymmetrically pyrazole-3-carboxylic acid substituted phthalocyanine-based photoanodes for use in water splitting photoelectrochemical and dye-sensitized solar cells. Solar Energy 2019; 191: 654-662.
12. Sarı FA, Kazıcı M, Harputlu E, Bozar S, Koyun Ö et al. Zn phthalocyanine derivatives for solution-processed small molecule organic solar cells. Chemistry Select 2018; 3: 13692-13699.
13. Hohnholz D, Steinbrecher S, Hanack M. Application of phthalocyanines in organic light emitting devices. Jornal of Moleculer Structures 2000; 521: 231-237.
14. Özmen ÖT, Goksen K, Demir A, Durmuş M, Köysal O. Investigation of photoinduced change of dielectric and electrical properties of indium (III) phthalocyanine and fullerene doped nematic liquid crystal. Synthetic Metals 2012; 162: 2188-2192.
15. Li Y, Tao X, Wei J, Lv X, Wang HG. Metal phthalocyanine-porphyrin-based conjugated microporous polymer-derived bifunctional electrocatalysts for zn-air batteries. Chemistry-An Asian Journal 2020; 15: 1970-1975.
16. Bıyıklıoğlu Z, Sofuoğlu A. Peripherally and non-peripherally electropolymerizable (2-{2-[4-(1H-pyrrol-1-yl)phenoxy]ethoxy}ethoxy) group substituted cobalt(II), manganese(III) phthalocyanines: Synthesis and electrochemistry. Journal of Molecular Structure 2020; 1212: 128144.
17. Olgac R, Soganci T, Baygu Y, Gök Y, Ak M. Zinc(II) phthalocyanine fused in peripheral positions octa-substituted with alkyl linked carbazole: Synthesis, electropolymerization and its electro-optic and biosensor application. Biosensors and Bioelectronics 2017; 98: 202-209.
18. Keleş T, Barut B, Bıyıklıoğlu Z, Özel A. A comparative study on DNA/BSA binding, DNA photocleavage and antioxidant activities of water soluble peripherally and non-peripherally tetra-3-pyridin-3-ylpropoxy-substituted Mn(III), Cu(II) phthalocyanines. Dyes and Pigments 2017; 139: 575-586.
19. Sen P, Sindelo A, Mafukidze DM, Nyokong T. Synthesis and photophysicochemical properties of novel axially di-substituted silicon (IV) phthalocyanines and their photodynamic antimicrobial chemotherapy (PACT) activity against Staphylococcus aureus. Synthetic Metals 2019; 258: 116203.
20. Barut B, Sofuoğlu A, Bıyıklıoğlu Z, Özel A. The water soluble peripherally tetra-substituted zinc (II), manganese (III) and copper (II) phthalocyanines as new potential anticancer agents. Dalton Transactions 2016; 45: 14301-14310.
21. Barut B, Bıyıklıoğlu Z, Yalçın CÖ, Abudayyak M. Non-aggregated axially disubstituted silicon phthalocyanines: Synthesis, DNA cleavage and in vitro cytotoxic/phototoxic anticancer activities against SH-SY5Y cell line. Dyes and Pigments 2020; 172: 107794.

22. Bıyıklıoğlu Z, Barut B, Özel A. Synthesis, DNA/BSA binding and DNA photocleavage properties of water soluble BODIPY dyes. Dyes and Pigments 2018; 148: 417-428.

23. Çakır D, Göksel M, Çakır V, Durmuş M, Bıyıklıoğlu Z. Amphiphilic zinc phthalocyanine photosensitizers: synthesis, photophysicochemical properties and in vitro studies for photodynamic therapy. Dalton Transactions 2015; 44: 9646-9658.

24. Akyüz D, Keleş T, Bıyıklıoğlu Z, Koca A. Metallophthalocyanines bearing polymerizable {[5-({(1E)-[4-(diethylamino)phenyl]methylene} amino)-1-naphthy1]oxy} groups as electrochemical pesticide sensor. Electroanalysis 2017; 29: 2913-2924.

25. Bıyıklıoğlu Z, Sofuoğlu A. Synthesis and electropolymerization properties of [(4-{3-[3-

(dimethylamino)phenoxy]propoxy}phenyl)metoxy] and [(4-{3-[3- (diethylamino)phenoxy]propoxy}phenyl)metoxy] substituted silicon naphthalocyanines. Journal of Molecular Structure 2017; 1148: 15-21.

26. Bıyıklıoğlu Z. New water soluble and amphiphilic titanium(IV) phthalocyanines and investigation of electropolymerization properties. Journal of Organometallic Chemistry 2014; 752: 59-66.

27. Bıyıklıoğlu Z, Çakır D. New electropolymerizable metal-free and metallophthalocyanines bearing {2,3-bis[3-(diethylamino)phenoxy] propoxy} substituents. Dyes and Pigments 2014; 100: 150-157.

28. Sen P, Yıldız SZ. Substituted manganese phthalocyanines as bleach catalysts: synthesis, characterization and the investigation of de-aggregation behavior with LiCl in solutions. Research on Chemical Intermediates 2019; 45: 687-707.

29. Bıyıklıoğlu Z, Çakır V, Demir F, Koca A. New electropolymerizable metal-free and metallophthalocyaninesbearing {2-[3-(diethylamino) phenoxy]ethoxy} substituents. Synthetic Metals 2014; 196: 166-172.

30. Bıyıklıoğlu Z, Alp H. Electropolymerizable peripherally tetra-{2-[3-(diethylamino)phenoxy]ethoxy} substituted as well as axially (4-phenylpiperazin-1-yl)- propanoxy-disubstituted silicon phthalocyanines and their electrochemistry. Dalton Transactions 2015; 44: 18993-18999.

31. Baş H, Bıyıklıoğlu Z. Synthesis and electropolymerization properties of new axially substituted subphthalocyanines bearing polymerizable 2-[4-({(1E)-[4- (dimethylamino,diethylamino)phenyl]methylene}amino)phenyl]ethoxy groups. Inorganica Chimica Acta 2017; 467: 56-61.

32 Bıyıklıoğlu Z, Baş H. Synthesis and effect of substituent position, metal type on the electrochemical properties of (3-morpholin-4-ylpropoxy) groups substituted cobalt, manganese phthalocyanines. Turkish Journal of Chemistry 2020; 44: 687-694.

33. Çakır V, Kantekin H, Bıyıklıoğlu Z, Koca A. New electropolymerizable metal-free, metallophthalocyanines and their electrochemical, spectroelectrochemical studies. Journal of Organometallic Chemistry 2014; 768: 28-35.

34. Göktuğ Ö, Soğancı T, Ak M, Sener MK. Efficient synthesis of EDOT modified ABBB-type unsymmetrical zinc phthalocyanine: optoelectrochromic and glucose sensing properties of its copolymerized film. New Journal of Chemistry 2017; 23: 14080-14087.

35. Akyüz D, Demirbaş Ü, Koca A, Çelik F, Kantekin H. Electrochemistry, electropolymerization and electrochromism of novel phthalocyanines bearing morpholine groups. Journal of Molecular Structure 2020; 1206: 127674

SUPPLEMENTARY INFORMATION

1. Materials and equipment

4-(diethylamino)-2-hydroxybenzaldehyde and 3-nitrophthalonitrile were purchased from commercial suppliers. All reagents and solvents were of reagent grade quality and were obtained from commercial suppliers. The IR spectra were recorded on a Perkin Elmer 1600 FT-IR spectrophotometer using KBr pellets. ^{1}H and ^{13}C-NMR spectra were recorded on a Bruker Avance III 400 MHz spectrometers in DMSO-d_6 and chemical shifts were reported (δ) relative to Me_4Si as an internal standard. MALDI-MS of complexes were obtained in dithranol (DIT), α-cyano-4-hydroxycinnamic acid (CHCA) as MALDI matrices using nitrogen laser accumulating 50 laser shots using Bruker Microflex LT MALDI-TOF mass spectrometer (Bremen, Germany). Optical spectra in the UV-vis region were recorded with a Perkin Elmer Lambda 25 spectrophotometer.

2. Electrochemical measurements

The cyclic voltammetry (CV) and square wave voltammetry (SWV) measurements were carried out with Gamry Interface 1000 potentiostat/galvanostat controlled by an external Pc and utilizing a three-electrode configuration at 25 °C. The working electrode was a Pt disc with a surface area of 0.071 cm^2. A Pt wire served as the counter electrode. Saturated calomel electrode (SCE) was employed as the reference electrode and separated from the bulk of the solution by a double bridge. Electrochemical grade TBAP in extra pure DCM was employed as the supporting electrolyte at a concentration of 0.10 mol dm^{-3}.

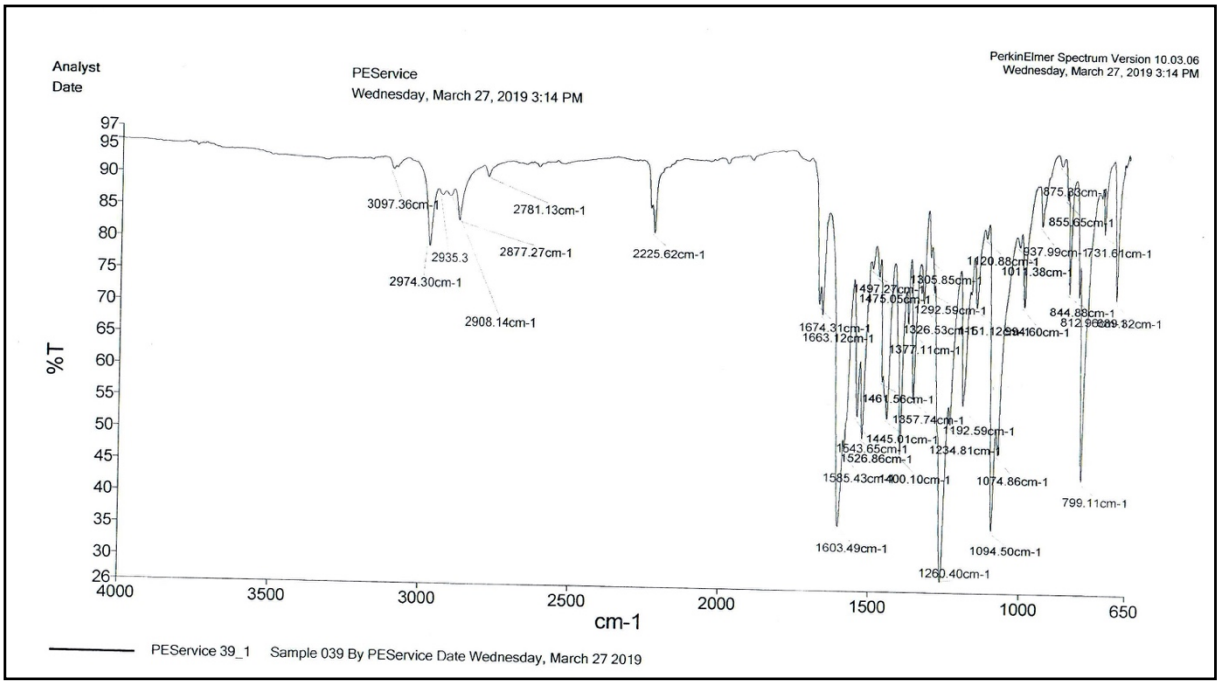

Figure S1. IR spectra of **n-TY-CN**.

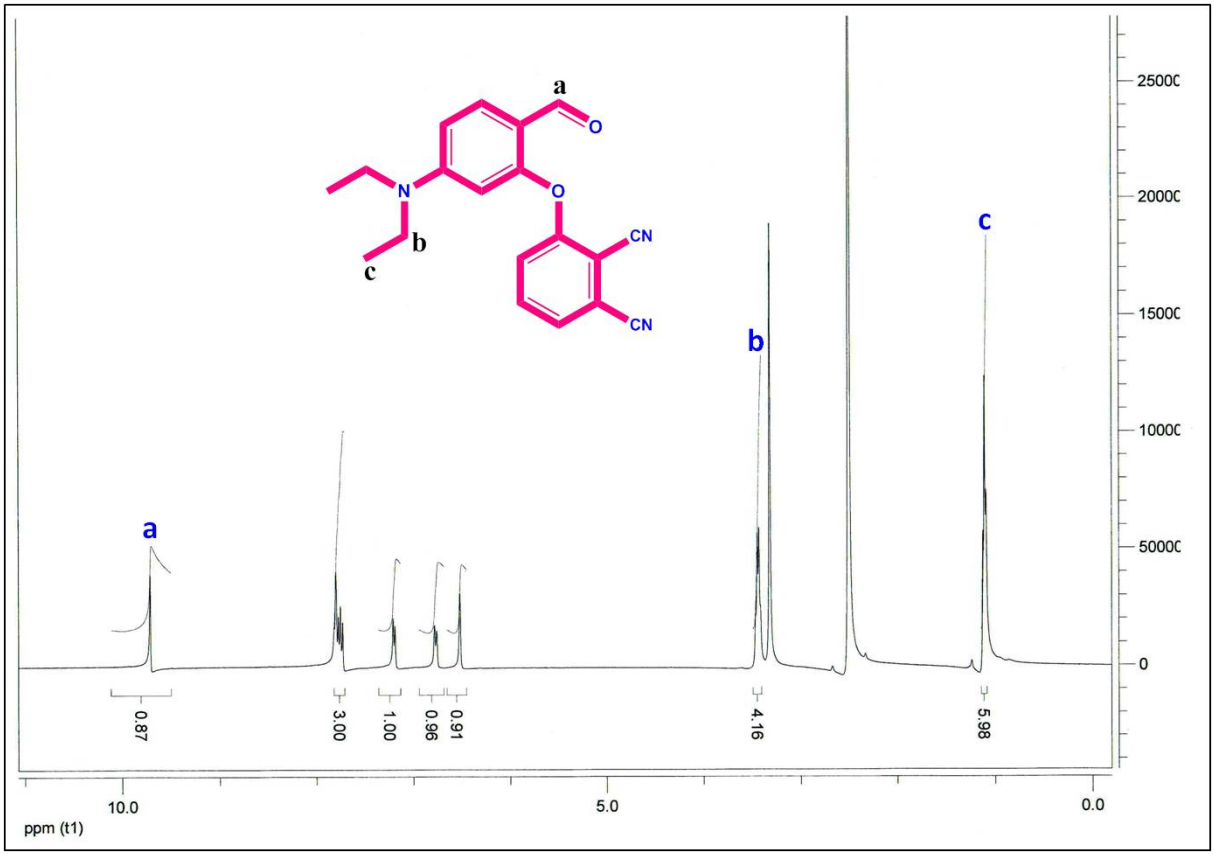

Figure S2. ^{1}H-NMR spectrum of **n-TY-CN** in DMSO-d$_6$.

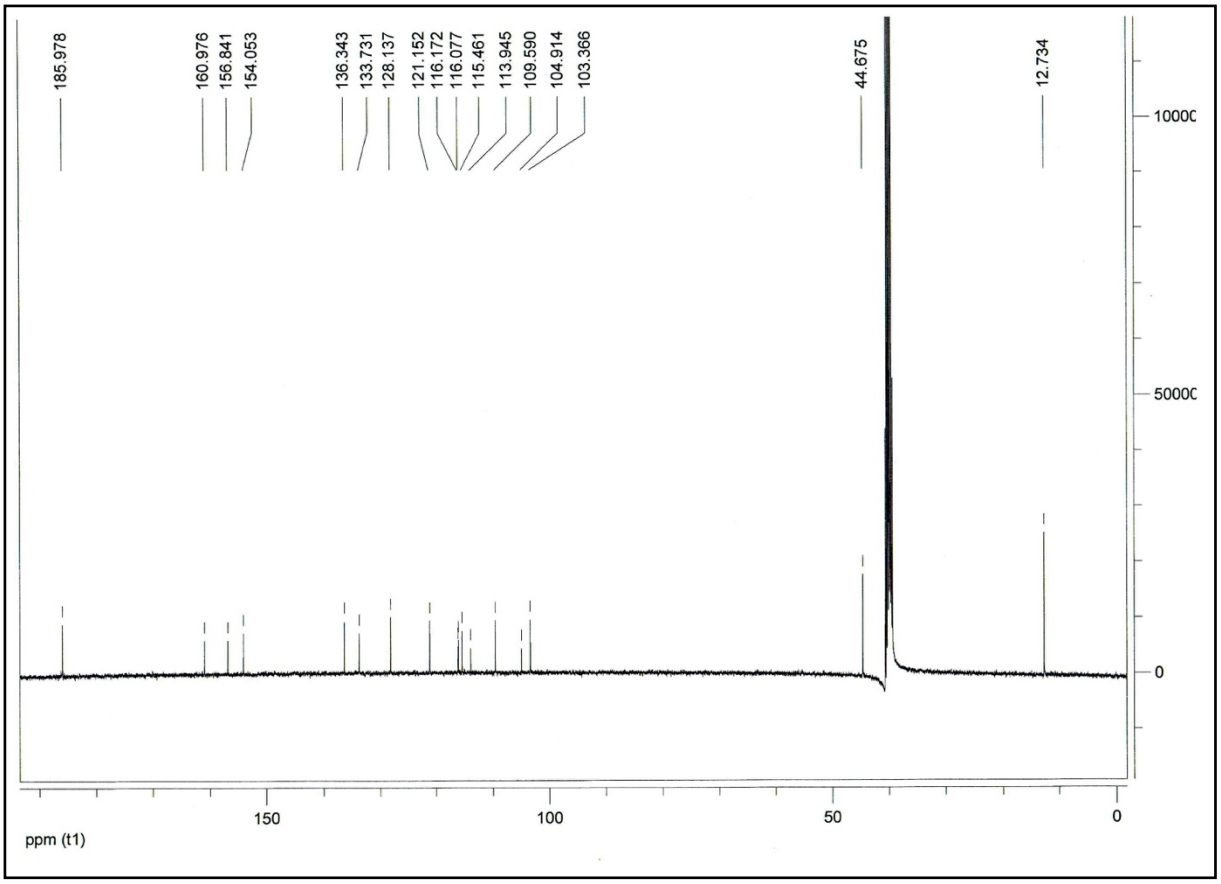

Figure S3. ^{13}C-NMR spectrum of **n-TY-CN** in DMSO-d$_6$.

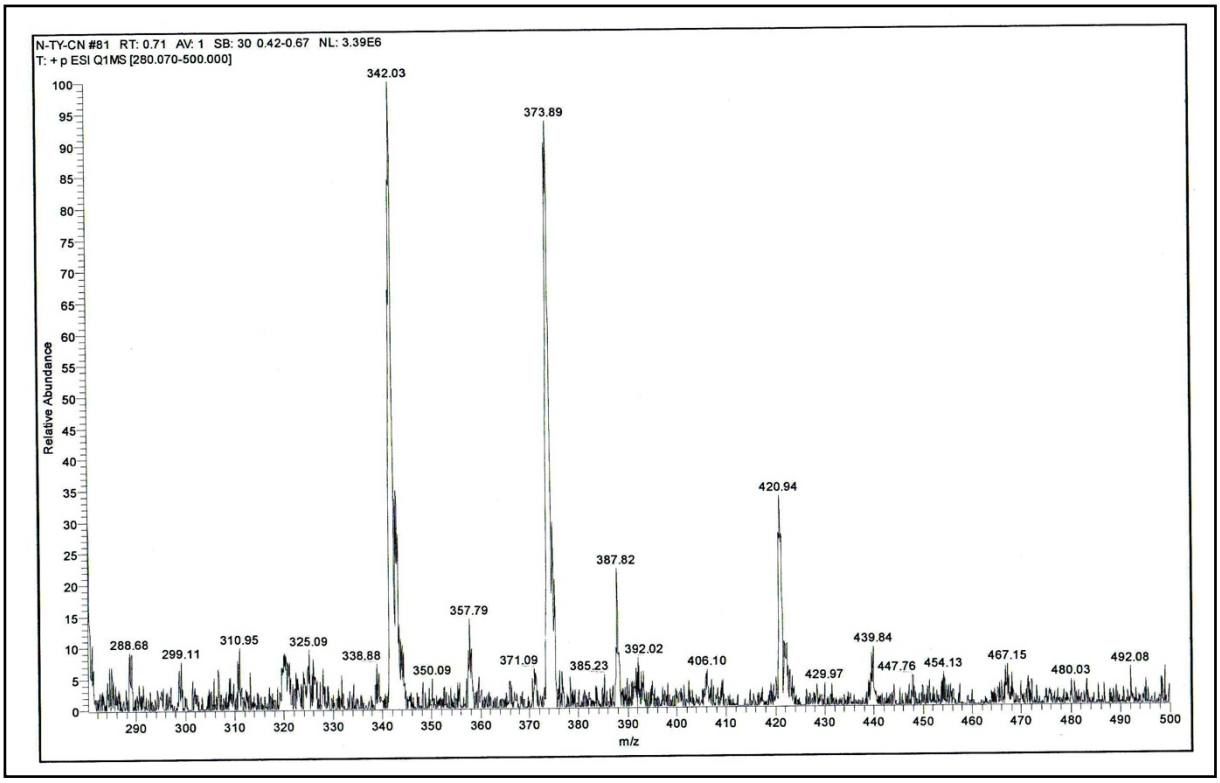

Figure S4. Mass of **n-TY-CN**.

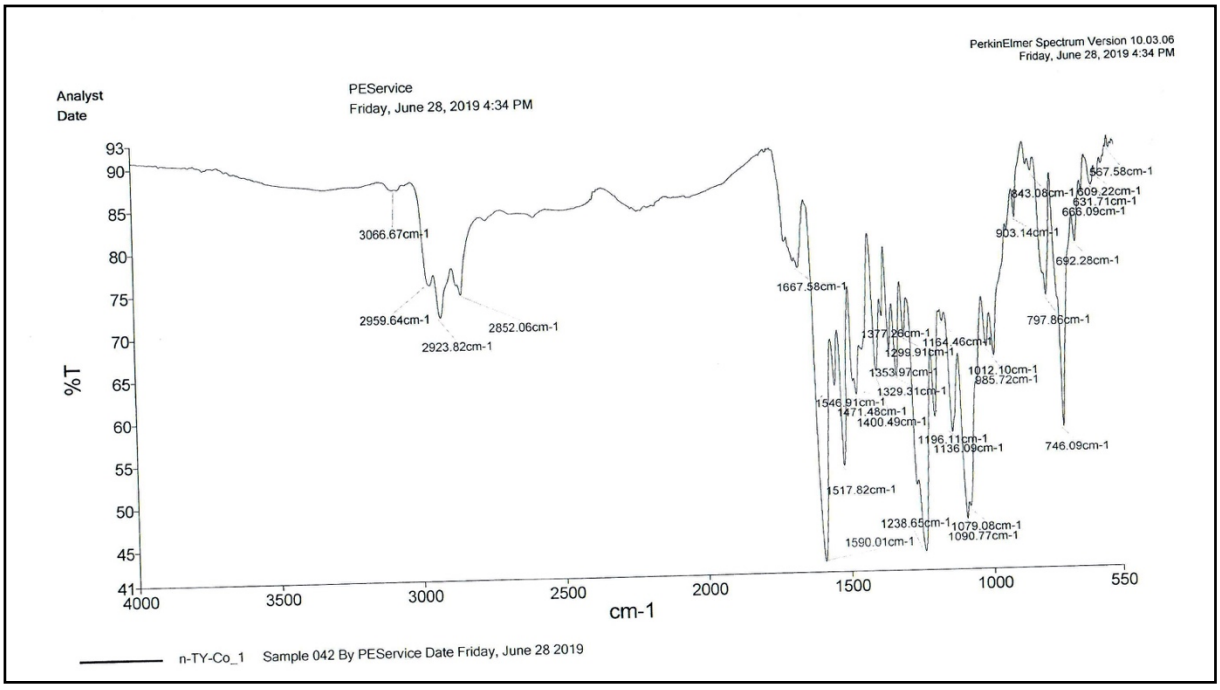

Figure S5. IR spectra of **n-TY-Co**.

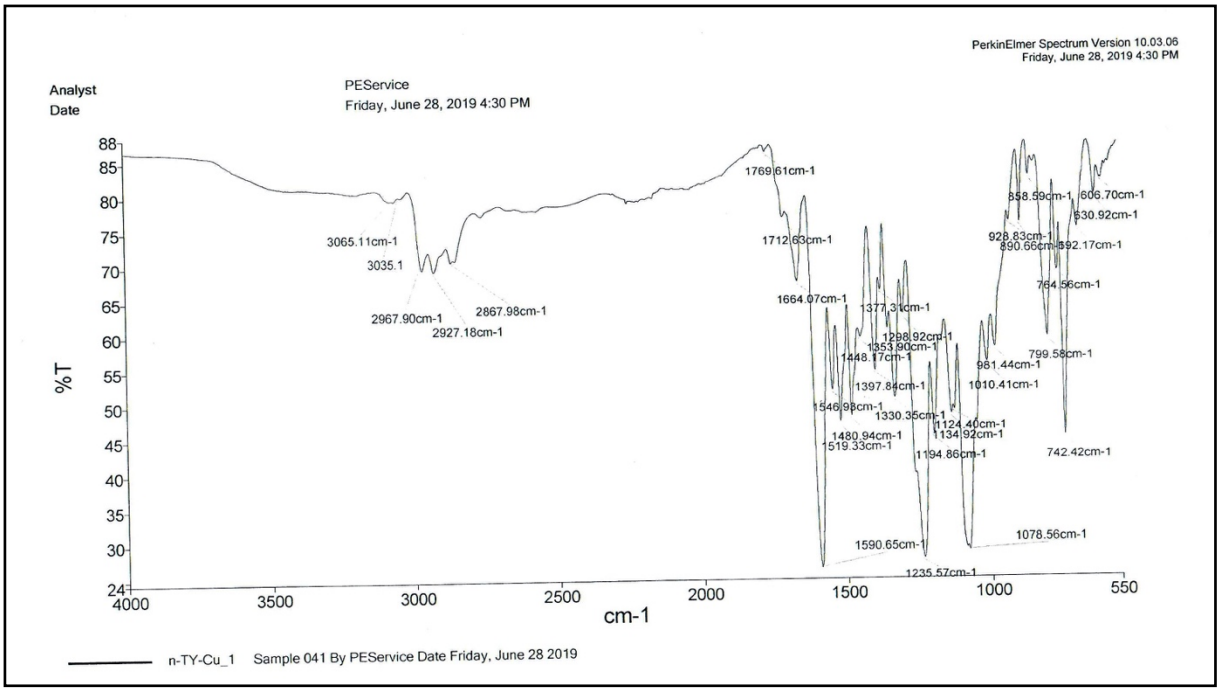

Figure S6. IR spectra of **n-TY-Cu**.

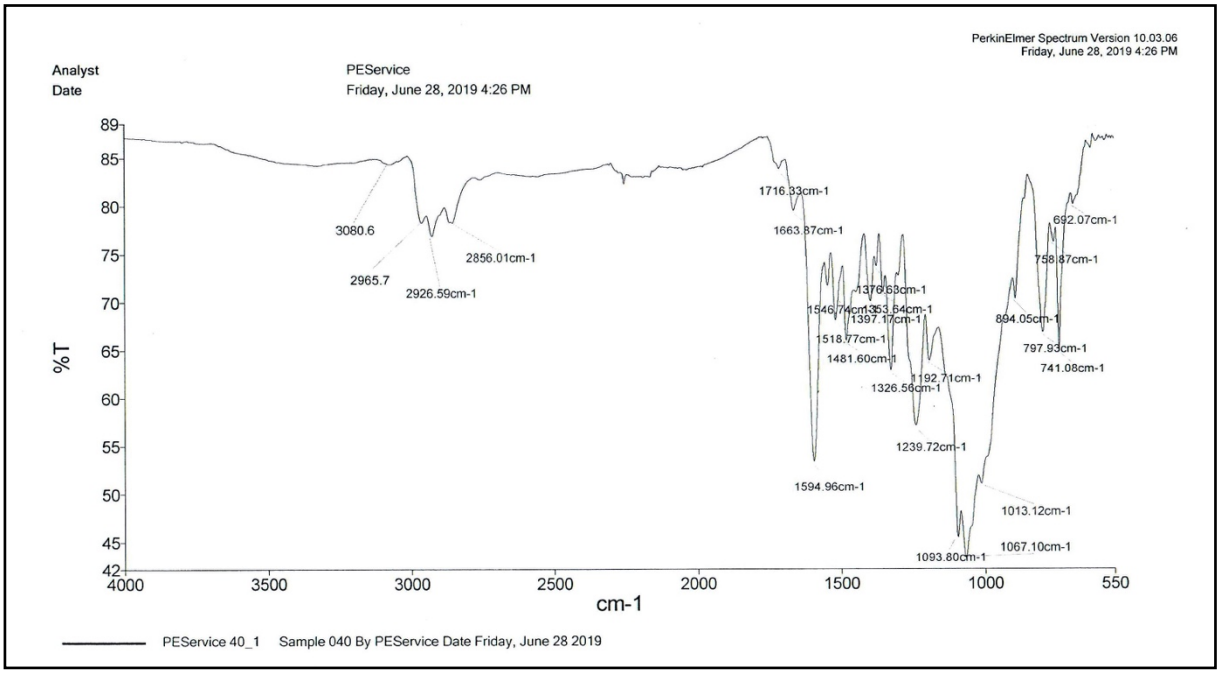

Figure S7. IR spectra of **n-TY-Mn**.